



Integrity performance characterization of BeiDou B1C and B2a signal-in-space error

Liying Huo¹ · Jiawen Shen¹ · Shizhuang Wang¹ · Yawei Zhai¹ · Xingqun Zhan¹ 

Received: 21 May 2023 / Revised: 23 August 2023 / Accepted: 27 August 2023 / Published online: 11 September 2023
© Shanghai Jiao Tong University 2023

Abstract

Global Navigation Satellite System (GNSS) Signal-In-Space (SIS) quality directly affects positioning integrity, which is an important metric for safety-critical applications. BeiDou Global Navigation Satellite System (BDS-3) broadcasts two new signals interoperable with GPS and Galileo, i.e., B1C and B2a. They are expected to serve civil aviation applications, following the Standards and Recommended Practices (SARPs) released by International Civil Aviation Organization (ICAO). Therefore, the SIS accuracy and integrity performance of BDS-3 B1C and B2a are evaluated in this work. The SIS Range Errors (SISREs) are achieved by comparing the broadcast satellite positions and clock offsets derived from Civil Navigation Message (CNAV) with the precise products from International GNSS Service (IGS). Specifically, given that the IGS precise products are referring to the equivalent phase center of BeiDou Regional System (BDS-2) B1I + B3I ionosphere-free combination, Differential Code Bias (DCB) from IGS is applied to realize time synchronization. This synchronization method is also meaningful to different frequencies in other constellations and supports the en-route, approaching, and landing phases. By analyzing 1-year data, an overall SIS characteristic picture of the 18 BDS-3 MEO satellites is presented here. The results show that most BDS-3 satellites are subject to an overbounding User Range Accuracy (URA) of 0.5 m to 0.85 m and a fault probability of 1.4953×10^{-5} to 1.1975×10^{-4} , with an integrity performance much better than that of BDS-2 and comparable to that of GPS. BDS-3 is now ready to serve civil aviation and other safety-critical applications.

Keywords Global Navigation Satellite System · Signal-in-space · BDS-3 · Integrity performance

1 Introduction

GNSS has become an indispensable aspect of various industries and daily life. In June 2020, the BDS-3 reached its full operation after the persistent and consistent regional service of BDS-2 [1, 2]. It provides high-accuracy positioning, navigation, and timing (PNT) services to global users in all weathers. Aviation and other safety-critical applications have emerged as crucial areas for the utilization of BDS-3 [3].

The modernization and upgrade of BDS-3 signals have been carried out in compliance with users' requirements. These new signals, namely B1C [4] and B2a [5], are an important feature of BDS-3. They are interoperable with GPS and Galileo. Specifically, B1C and B2a signals are enhanced to support Dual-Frequency Multi-Constellation (DFMC)

satellite-based augmentation system services [6]. According to International Civil Aviation Organization (ICAO) guidelines, B1C, B2a, and B1I are intended for civil aviation, and are expected to comply with Standards and Recommended Practices (SARPs).

Accuracy and integrity assessment are critical for BDS-3 to serve civil aviation. Integrity is mainly to measure the reliability of GNSS, indicating the ability to provide timely warnings to users when the navigation system is unavailable. SIS quality significantly impacts user positioning accuracy and integrity, where SIS Range Error (SISRE) is a crucial variable that affects accuracy and integrity [7]. SISRE describes the equivalent pseudorange error originating from satellite ephemeris and clock errors. The nominal and anomalous behaviors of SISRE are defined by the Integrity Support Message (ISM) [8]. ISM is a critical input of Advanced Receiver Autonomous Integrity Monitoring (ARAIM) [9–11], including User Range Accuracy (URA) and prior fault probability.

✉ Xingqun Zhan
xqzhan@sjtu.edu.cn

¹ Shanghai Jiao Tong University, Shanghai, China

Various studies have been conducted to evaluate the SIS accuracy and integrity for different constellations. The instantaneous SIS error was analyzed for GPS and GLONASS, and appropriate upper bounds for probable distribution were established [12, 13]. A method including the group delay error model in ARAIM was described, and a novel model of URA bounding for Galileo was presented [14]. An SISRE analysis was conducted on all available constellations from 2013 to 2014 [15]. This analysis was subsequently broadened to include the evaluation criteria of other constellations and extended to 2017 [16]. For BDS, long-term behavior and statistical characterization of BDS-2 SIS errors were obtained [7]. And similar analysis was carried out for BDS-3 [17]. A further comparison of SISRE between BDS-3 and BDS-2 was presented later [18].

By far, SIS integrity assessments for BDS-3 are limited. Wang et al. presented an evaluation method for SISRE that aligned with safety standards and employed it to analyze the performance of BDS B1I/B3I [19]. Our prior work emphasized integrity and introduced a data-driven evaluation scheme. However, the integrity performance of B1C and B2a should be further addressed, since they are critical new signals in BDS-3 serving as important interoperable signals specifically for aviation. Based on the methodologies developed in [19], the calculation of SISREs involves a comparison between the satellite positions and clock offsets calculated from the Civil Navigation Message (CNAV) and the precise products supplied by the International GNSS Service (IGS). Different from [19], the IGS precise products pertain to the equivalent phase center of the B1I + B3I ionosphere-free (IF) combination, and the Differential Code Bias (DCB) products from IGS are necessary for time synchronization. By analyzing 1 year data from 18 Medium Earth Orbit (MEO) satellites, the SIS integrity performance of BDS-3 B1C and B2a signals is characterized.

The rest of this paper is organized as follows: Sect. 2 introduces the data used in the evaluation of this article, and Sect. 3 describes the calculation method of SISRE, which includes the derivation of clock correction equations for B1C and B2a in detail. Section 4 presents the evaluation results and analysis of them. The conclusion is given in Sect. 5.

2 Data

To characterize the integrity performance of SIS for BDS, the collection, processing, and calculation of broadcast ephemerides (BCEs), precise ephemerides (PCEs), and DCB data are essential. By evaluating relevant SISRE, the SIS integrity performance can be characterized.

BCEs and PCEs are provided by the International GNSS Monitoring and Assessment System (IGMAS) and IGS Multi-GNSS Experiment (MGEX). BCEs include orbit and

clock error parameters for GPS, GLONASS, Galileo, BDS, and other systems. The commonly used BCEs are the Legacy Navigation Message (LNAV) files and the p-type files of the Receiver Independent Exchange Format (RINEX). The investigation of B1C/B2a signals requires the inclusion of CNAV files [20]. The final PCEs are released 12–19 days after the BCEs broadcast, with the highest accuracy. In navigation research, the final PCEs are widely used as the true position of the satellite.

DCB is a time-delay-like hardware delay or code bias difference generated by various GNSS signals in different channels of satellites and receivers. The reference for GNSS satellite clock bias is typically designated by a specified frequency, such as BDS-2 B3I, or by an ionosphere-free combination of two frequencies, such as GPS P1/P2 and Galileo E1/E5a pseudorange observations. Therefore, when utilizing disparate frequencies and observation combinations, it becomes necessary to incorporate a DCB for bias correction [21].

The BDS B1C/B2a CNAV files were sourced from the China Satellite Navigation Office (CSNO). However, the CNAV files only covered a period of 19 days in the year 2020. This limitation of data constrained our ability to analyze the system. Consequently, we focused on analyzing the data from 2021. Despite the limited data, we were still able to extract valuable information regarding the integrity performance of BeiDou B1C/B2a from the files of 2021. In the future, we will delve deeper into BDS integrity analysis using longer term and more up-to-date data. The data of the year 2021 mainly include the following:

- 1) BCEs (CNAV): BDS CNAV BCEs, were downloaded from the Test and Evaluation Research Center of the China Satellite Navigation System Management Office.
- 2) PCEs: precise orbits and precise clocks, were analyzed using the German Geoscience Research Center (GFZ) and WHU analysis centers, and final products were used as the data products.
- 3) DCB data: DCB precise products, were downloaded from the Chinese Academy of Sciences.

3 Methodology

The SIS integrity performance assessment process is illustrated in Fig. 1 and comprises three distinct phases. First, space–time unification procedures are performed for BCE and PCE to compute the broadcast orbital error and broadcast clock error. Subsequently, the calculated broadcast orbital and broadcast clock errors are projected to the line-of-sight direction to generate the SISRE. Finally, a Gaussian distribution is used to describe SISRE from an integrity perspective.

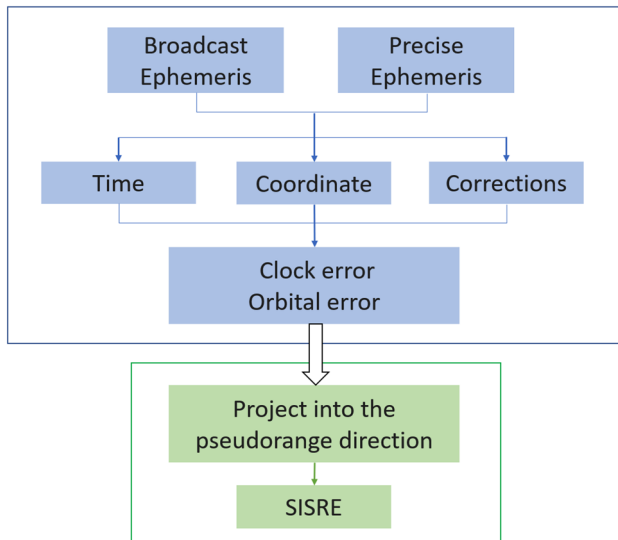


Fig. 1 BDS SIS integrity performance assessment algorithm flow

It is necessary to unify the time and coordinate systems to ensure that the comparison between BCEs and PCEs is consistent. In particular, the dual-frequency clock error correction equation is derived using Time Group Delay (TGD) and DCB. The subsequent sections provide an overview of the data preprocessing procedures before the computation of SISRE.

3.1 Time

Regarding time reference processing, PCEs utilize GPS time (GPST) as the time scale, while BCEs utilize BDS time (BDT). In this paper, GPST is chosen as the fundamental time scale, and a 14 s BDT-GPST time offset is selected for the broadcast ephemerides. Although a possible synchronization error of around 50 ns between GPST and BDT will show up, it can be disregarded when comparing BCE and PCE [22].

3.2 Coordinate

In processing of coordinate system unification, precise orbit uses the International Terrestrial Reference Frame 2008 (ITRF2008) coordinate system, while the broadcast orbit of BDS adopts China Geodetic Coordinate System 2000 (CGCS2000). As the centimeter level coordinate difference between CGCS2000 and ITRF2008 is much lower than the error of BCE, it can be ignored in correlation analysis [23]. The results of the positioning for the two coordinate systems are compatible. Nevertheless, when BDS calculates satellite coordinates with broadcast ephemeris parameters, it must utilize the associated earth gravitational constant, reference ellipsoidal flattening, and earth rotation angular

velocity. Otherwise, solutions for satellite coordinates will produce errors that measure in meters [24].

3.3 Corrections

According to the IGS convention, all PCEs provide the orbit positions of the satellite Center of Mass (CoM), while the corresponding parameters of BCEs are referred to Antenna Phase Center (APC) [25]. The fact is that a direct comparison between the coordinate of PCEs and the coordinate of BCEs is not feasible, and proper Phase Center Offset (PCO) correction, which describes the position of the satellite’s APC concerning its CoM must be proposed before the calculation of satellite SIS User Range Error (URE) [26].

The broadcast orbital errors of Earth-Centered Earth-Fixed (ECEF) solid coordinate system, namely, $[\Delta x \ \Delta y \ \Delta z]^T$, are calculated as follows:

$$\begin{bmatrix} \Delta x \\ \Delta y \\ \Delta z \end{bmatrix} = \begin{bmatrix} x \\ y \\ z \end{bmatrix}_b - \left(\begin{bmatrix} x \\ y \\ z \end{bmatrix}_p - A_S^E \cdot \begin{bmatrix} dx \\ dy \\ dz \end{bmatrix}_{PCO} \right), \quad (1)$$

where A_S^E is the attitude matrix describing the transformation from the satellite-fixed frame to ECEF, dx , dy , and dz represent PCOs, and subscripts “ b ” and “ p ” mean the BCEs and PCEs, respectively.

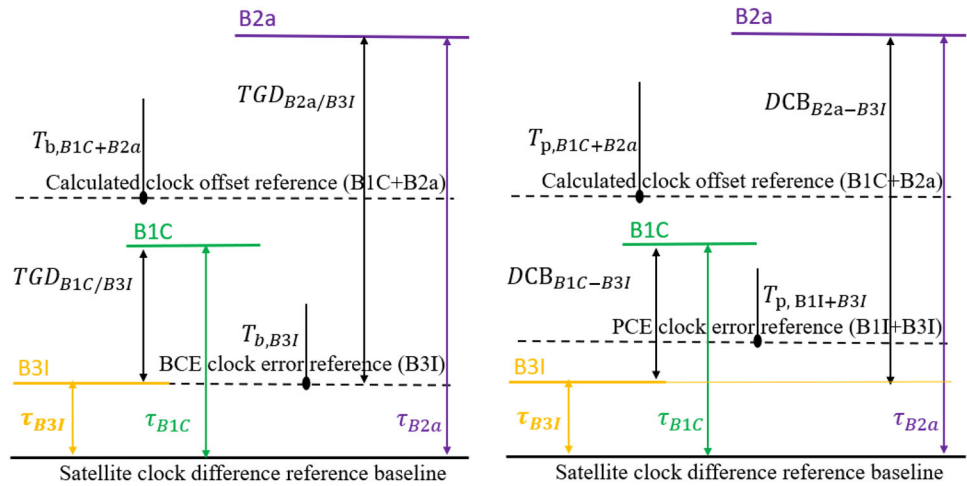
The difference between broadcast clock offset and precise clock offset can be given by the following equation:

$$\delta T_b^i = T_b^i - T_p^i. \quad (2)$$

However, given the fact that the precise clocks are referring to the APC of B1I + B3I IF, while the broadcast clocks are referring to the APC of B3I, time synchronization is a must-do before computing the clock error based on Eq. (2). The DCB between signals of different frequencies is called inter-frequency difference, and TGD also belongs to inter-frequency difference. GNSS broadcasts TGD or other time delay parameters in the BCE. TGD is an important factor affecting positioning and timing accuracy. Aviation users employ the TGD to compute the satellite clock offsets referred to the APC of B1C + B2a IF. In contrast, the DCB parameters obtained from IGS are more accurate than TGD and will be used to transform the reference point of the precise satellite clock offsets from the APC of B1I + B3I IF to the APC of B1C + B2a IF.

Figure 2 gives the composition of the broadcast clock offset and precise clock offset of the BDS and their time delays. On the satellite side, the clock reference for broadcasting the signal is called the satellite clock difference reference baseline (solid line at the bottom). For BDS, the time delays of B3I, B1C, and B2a from signal generation to emission

Fig. 2 TGD/DCB and broadcast/precise satellite clock offset parameters



based on the same clock difference reference baseline are τ_{B3I} , τ_{B1C} , τ_{B2a} (colorful solid line with double arrows), the inter-frequency deviation of B1C and B3I is $TGD_{B1C/B3I}$ (black solid line with double arrows), and the same for other TGD/DCB parameters. Dashed lines indicate different clock references. Black solid lines with a dot mean clock offset ($T_{b/p, B1C+B2a}$) or error ($T_{b/p, B3I/B1I+B3I}$). The left figure represents TGD and broadcast satellite clock offset parameters, and the right one represents DCB and precise satellite clock offset parameters.

The broadcast clock offset of the BDS satellite i is denoted as $T_{b, B3I}^i$ based on the APC of the B3I signal, while the precise clock offset based on the equivalent APC of B1I/B3I IF is denoted as $T_{p, B1I+B3I}^i$. Therefore, TGD is needed to correct the broadcast clock offset to compare BCE with PCE. In addition, to analyze the clock deviation error on the B1C/B2a IF, the precise clock offset needs to be corrected by DCB [26].

The broadcast clock offset $T_{b, B1C+B2a}^i$ of BDS B1C/B2a can be calculated as

$$T_{b, B1C+B2a}^i = T_{b, B3I}^i - \frac{f_{B1C}^2}{f_{B1C}^2 - f_{B2a}^2} TGD_{B1C/B3I}^i + \frac{f_{B2a}^2}{f_{B1C}^2 - f_{B2a}^2} TGD_{B2a/B3I}^i, \quad (3)$$

where f_{B1C} and f_{B2a} are the frequency of B1C and B2a, respectively, and $TGD_{B1C/B3I}^i$ and $TGD_{B2a/B3I}^i$ are the TGD values of B1C and B2a relative to B3I, respectively.

The precise clock offset $T_{p, B3I}^i$ of BDS B3I can be calculated as

$$T_{p, B3I}^i = T_{p, B1I+B3I}^i + \frac{f_{B1I}^2}{f_{B1I}^2 - f_{B3I}^2} DCB_{B1I-B3I}^i, \quad (4)$$

where $DCB_{B1I-B3I}^i$ is the DCB value of B1I relative to B3I.

The precise clock offset $T_{p, B1C+B2a}^i$ of BDS B1C/B2a can be calculated as

$$T_{p, B1C+B2a}^i = T_{p, B3I}^i - \frac{f_{B1C}^2}{f_{B1C}^2 - f_{B2a}^2} DCB_{B1C-B3I}^i + \frac{f_{B2a}^2}{f_{B1C}^2 - f_{B2a}^2} DCB_{B2a-B3I}^i, \quad (5)$$

where $DCB_{B1C-B3I}^i$ and $DCB_{B2a-B3I}^i$ are the DCB values of B1C and B2a relative to B3I, respectively.

Thus, the difference between the broadcast clock offset and the precise clock offset of BDS B1C/B2a is described as

$$\begin{aligned} \delta T_{b, B1C+B2a}^i &= T_{b, B1C+B2a}^i - T_{p, B1C+B2a}^i \\ &= T_{b, B3I}^i - \frac{f_{B1C}^2}{f_{B1C}^2 - f_{B2a}^2} TGD_{B1C/B3I}^i + \frac{f_{B2a}^2}{f_{B1C}^2 - f_{B2a}^2} TGD_{B2a/B3I}^i - T_{p, B1I+B3I}^i \\ &\quad - \frac{f_{B1I}^2}{f_{B1I}^2 - f_{B3I}^2} DCB_{B1I-B3I}^i + \frac{f_{B1C}^2}{f_{B1C}^2 - f_{B2a}^2} DCB_{B1C-B3I}^i \\ &\quad - \frac{f_{B2a}^2}{f_{B1C}^2 - f_{B2a}^2} DCB_{B2a-B3I}^i. \end{aligned} \quad (6)$$

In addition, the reference clock of PCE has a time-varying and satellite-independent timescale bias μ (relative to GPST). Therefore, in the epoch of $\Delta T^i(k)$, the broadcast clock difference of satellite i can be modeled as

$$\Delta T^i(k) = \delta T_b^i(k) - \mu(k). \quad (7)$$

Table 1 Space–time unification parameters

	Broadcast ephemeris	Precise ephemeris	After correction
Time	BDT	GPST	GPST-BDT = 14(s)
Coordinate	CGS2000	ITRF	Centimeters level, ignored
Orbit error	APC of B3I	COM	$[\Delta x \Delta y \Delta z]^T = [xyz]_b^T - ([xyz]_p^T - A_S^E \bullet [dxdydz]_{PCO}^T)$
Clock error	APC of B3I	B1I + B3I	$\Delta T_{B1C+B2a} = T_{b, B3I} - \frac{f_{B1C}^2}{f_{B1C}^2 - f_{B2a}^2} TGD_{B1C/B3I} + \frac{f_{B2a}^2}{f_{B1C}^2 - f_{B2a}^2} TGD_{B2a/B3I} - T_{p, B1I+B3I} - \frac{f_{B1I}^2}{f_{B1I}^2 - f_{B3I}^2} DCB_{B1I-B3I}^i + \frac{f_{B1C}^2}{f_{B1C}^2 - f_{B2a}^2} DCB_{B1C-B3I}^i - \frac{f_{B2a}^2}{f_{B1C}^2 - f_{B2a}^2} DCB_{B2a-B3I}^i$

After a series of data preprocessing, we can get Table 1 to calculate SISRE.

3.4 Calculate SISRE

From the receiver end, the impact of the orbital error on the user pseudorange is the projection of the orbital error along line-of-sight (LOS), rather than the absolute value of the orbital error. And the clock deviation error is a scalar quantity, which is the same in all directions. The orbital error along LOS and the clock error is SIS User Range Error (SIS URE), or SISRE. The main calculation steps are as follows:

Furthermore, the clock deviation error maintains a uniform scalar quantity in all directions. The aggregation of both the orbital error along LOS and the clock error generates the SIS User Range Error (SIS URE), or SISRE. The process to compute the SISRE consists of the following calculation steps:

Radial (R), along-track (A), and cross-track (C) orbital errors are calculated as [27]

$$[\Delta e_R \ \Delta e_A \ \Delta e_C]^T = A_E^O \bullet [\Delta x \ \Delta y \ \Delta z]^T, \tag{8}$$

where $[\Delta x \ \Delta y \ \Delta z]^T$ represents the ECEF orbital error vector, and A_E^O is the transformation matrix from ECEF to the local orbital frame. Concerning a given satellite position r and an inertial velocity v in ECEF, the transformation matrix is determined as [12]

$$A_E^O = \left[\frac{r}{|r|} \ \frac{r \times v}{|r \times v|} \times \frac{r}{|r|} \ \frac{r \times v}{|r \times v|} \right]^T. \tag{9}$$

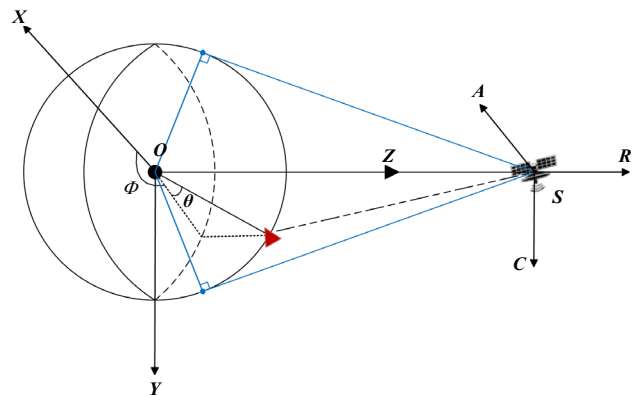


Fig. 3 Geometric method to calculate the IURE [19]

The characteristics of BCE errors can be evaluated and analyzed by calculating radial, along-track, and cross-track orbital errors.

The instantaneous URE (IURE) error refers to the equivalent pseudorange error that occurs within a specified period. Figure 3 displays the IURE geometric methodology employed in the calculation. This implementation adopts a geocentric coordinate system (O-XYZ) that aligns with the axis of the local orbital coordinate system (S-RAC). Regarding this system, the earth is assumed to be a regular sphere, with the centroid O representing the origin. The satellite is located at point S, while the Z-axis points directly toward S. Accordingly, the O-XYZ coordinate system changes its orientation to mirror the satellite in terms of the ECEF coordinate system. For users whose distance from the center of

the earth is d , the IURE will be [19]

$$IURE = -\frac{\begin{bmatrix} \Delta e_R & \Delta e_A & \Delta e_C \end{bmatrix}}{\sqrt{1 + \kappa^2 - 2\kappa \sin(\theta)}} \begin{bmatrix} \kappa - \sin(\theta) \\ \cos(\theta)\cos(\phi) \\ \cos(\theta)\sin(\phi) \end{bmatrix} + \Delta T. \quad (10)$$

SIS IURE is related to the user's geographical location. We use the user-grid URE method to evaluate SISRE performance and determine the overbounding URA of each monitored satellite [19]. From an integrity perspective, ranging errors are usually described by Gaussian models, which yield a conservative Gaussian distribution through the overbounding URA [12, 28]. When the orbital and clock errors have Gaussian distribution, the error distribution of each user obtained by this index will conform to the Gaussian distribution.

4 Results and analysis

To analyze the SIS integrity performance of B1C and B2a, this study uses the BCEs and PCEs from January 1, 2021, to December 31, 2021, for error analysis. The accuracy of BDS-3 orbit error, clock error, and SISRE are analyzed from an integrity perspective, and the fault probability is calculated.

4.1 Broadcast orbital and clock error evaluation

Following the PCO correction process, the orbital error vector is transformed from the ECEF coordinate system to radial (R), along-track (A), and cross-track (C) orbital errors. As specified in Sect. 3, we can compute the broadcast orbital and clock errors of B1C/B2a, as shown in Table 2. The results indicate the presence of a non-zero-mean value, while systematic error means measurements that vary in predictable ways. It is necessary to deduct the non-zero-mean value from the results to remove the systematic error, and the final errors are shown in Table 3. Based on these statistical findings, the BDS-3 broadcast orbital clock is highly accurate, ranging from the centimeters to the decimeters' level.

The orbital and clock error FCDF curves of BDS-3 are shown in Fig. 4. To make it clear, the x-axis is limited to ± 3 m, and the y-axis ranges from 10^{-5} to 1. The analysis reveals that most error distributions exhibit a Gaussian core, with greater variance in their tail data. For BDS-3, the BCEs' orbital errors of radial direction are smaller than those of along-track and cross-track. This observation can be attributed to the higher sensitivity of ground tracking station observations to radial changes, and the current along-track and cross-track mechanical models are not perfect enough. In addition, by Kepler's law, the precise determination of the

orbit rotation period can also estimate the semi-major axis (radial direction) with high precision. We observed significant errors in both the along-track and cross-track errors from the graph. Notably, it is crucial to recognize that the impact of along-track and cross-track orbital errors on SISRE is comparatively smaller than in the radial direction. Several strategies can be employed to enhance the accuracy of along-track and cross-track orbital errors [29, 30]. However, these methods fall outside the scope of our current research. Our task is to assess the broadcast ephemeris, and we cannot alter the performance of the broadcast ephemeris. Our main focus here is to analyze and evaluate the BDS integrity performance. The clock errors of C19–C23 are slightly larger. Removing the system error suggests that hydrogen clock satellites yield smaller errors than rubidium clock satellites, mainly due to the higher accuracy of hydrogen clocks.

4.2 SISRE and fault probability of satellite assessment

By generating a mesh user grid, calculating IURE, and removing systematic error in IURE, the FCDF curve is developed according to the zero-mean IURE distribution. Then, it is ready to see a Gaussian distribution that strictly overbounds all FCDF curves within a certain region. The FCDF plot of SISRE and its overbounding (blue line) are shown in Fig. 5. Each colored thin line represents the user's IURE distribution, with a blue line representing the overbounding Gaussian distribution.

In the existing studies, the threshold is usually given as $4.42 \times \sigma URA$, where σURA represents broadcast URA [13]. However, this study adopts a set of thresholds for integrity assessment [19]. This decision stems from a few key factors [19]: (a) there is uncertainty about whether the broadcast URA accurately captures the genuine error distribution, (b) the selected threshold value significantly impacts estimated URA and fault probability, which are crucial parameters, and (c) utilizing a set of thresholds yields a more comprehensive SISRE evaluation compared to reliance on a solitary threshold. Table 4 presents the integrity assessment outcomes of BDS-3 (B1C/B2a) in 2021.

Due to different satellite configurations, the threshold is also somewhat different, but all are limited to 3 m. Please note that these results are based on the assumption that there were no faults during data outages. Given the wide variation in satellite performance, it is recommended to set a different threshold for individual satellites in integrity monitoring rather than one single threshold.

It can be seen from Figs. 4 and 5 that the trend and magnitude of SISRE of a single satellite are consistent with the radial orbital error and clock error respectively, indicating that the satellite radial orbital error and clock error SISRE are the main contribution items of SISRE.

Table 2 2021 BDS-3 (B1C/B2a) orbital and clock error (systematic error not removed)

PRN	Clock type	Mean (m)				RMSE (m)			
		R	A	C	T	R	A	C	T
C19	RB	0.221	0.286	0.287	0.245	0.231	0.368	0.368	0.319
C20	RB	0.212	0.296	0.301	0.359	0.221	0.380	0.382	0.434
C21	RB	0.206	0.292	0.296	0.320	0.216	0.376	0.375	0.671
C22	RB	0.185	0.293	0.294	0.221	0.196	0.378	0.378	0.300
C23	RB	0.196	0.296	0.287	0.649	0.207	0.380	0.366	0.700
C24	RB	0.182	0.296	0.287	0.183	0.192	0.381	0.368	0.286
C25	H	0.062	0.240	0.255	0.398	0.079	0.314	0.334	0.460
C26	H	0.058	0.242	0.241	0.781	0.074	0.315	0.318	0.825
C27	H	0.061	0.243	0.254	0.447	0.077	0.313	0.334	0.509
C28	H	0.073	0.332	0.279	0.646	0.098	0.525	0.385	0.740
C29	H	0.056	0.247	0.251	0.701	0.071	0.318	0.330	0.749
C30	H	0.058	0.249	0.256	0.211	0.073	0.319	0.338	0.281
C32	RB	0.207	0.282	0.312	0.364	0.216	0.360	0.394	0.423
C33	RB	0.229	0.277	0.303	0.973	0.236	0.356	0.384	1.021
C34	H	0.072	0.243	0.247	0.799	0.089	0.317	0.328	0.842
C35	H	0.074	0.246	0.242	0.825	0.091	0.317	0.323	0.871
C36	RB	0.352	0.282	0.294	0.983	0.358	0.362	0.377	1.073
C37	RB	0.343	0.288	0.295	0.978	0.349	0.370	0.375	1.029

RB is rubidium clock, *H* is hydrogen clock

Table 3 2021 BDS-3 (B1C/B2a) orbital and clock error (systematic error removed)

PRN	Clock type	Mean (m)				RMSE (m)			
		R	A	C	T	R	A	C	T
C19	RB	0.054	0.278	0.287	0.226	0.068	0.356	0.368	0.297
C20	RB	0.051	0.287	0.301	0.210	0.065	0.367	0.382	0.284
C21	RB	0.050	0.281	0.296	0.229	0.065	0.361	0.375	0.630
C22	RB	0.052	0.284	0.294	0.210	0.066	0.366	0.378	0.291
C23	RB	0.051	0.296	0.287	0.207	0.068	0.380	0.366	0.282
C24	RB	0.049	0.295	0.287	0.182	0.065	0.377	0.368	0.285
C25	H	0.061	0.239	0.255	0.199	0.077	0.312	0.334	0.268
C26	H	0.058	0.240	0.241	0.210	0.073	0.313	0.318	0.282
C27	H	0.055	0.243	0.254	0.229	0.069	0.313	0.334	0.304
C28	H	0.068	0.333	0.278	0.234	0.092	0.525	0.385	0.388
C29	H	0.054	0.247	0.251	0.207	0.068	0.318	0.330	0.278
C30	H	0.055	0.247	0.256	0.211	0.069	0.318	0.338	0.281
C32	RB	0.049	0.279	0.312	0.204	0.064	0.355	0.394	0.268
C33	RB	0.046	0.271	0.303	0.229	0.061	0.347	0.384	0.320
C34	H	0.070	0.243	0.247	0.205	0.086	0.317	0.328	0.288
C35	H	0.072	0.246	0.242	0.215	0.088	0.317	0.322	0.296
C36	RB	0.047	0.282	0.294	0.352	0.063	0.361	0.377	0.459
C37	RB	0.047	0.287	0.295	0.251	0.065	0.366	0.375	0.333

Fig. 4 Radial (R), along-track (A), cross-track (C), and clock error distributions

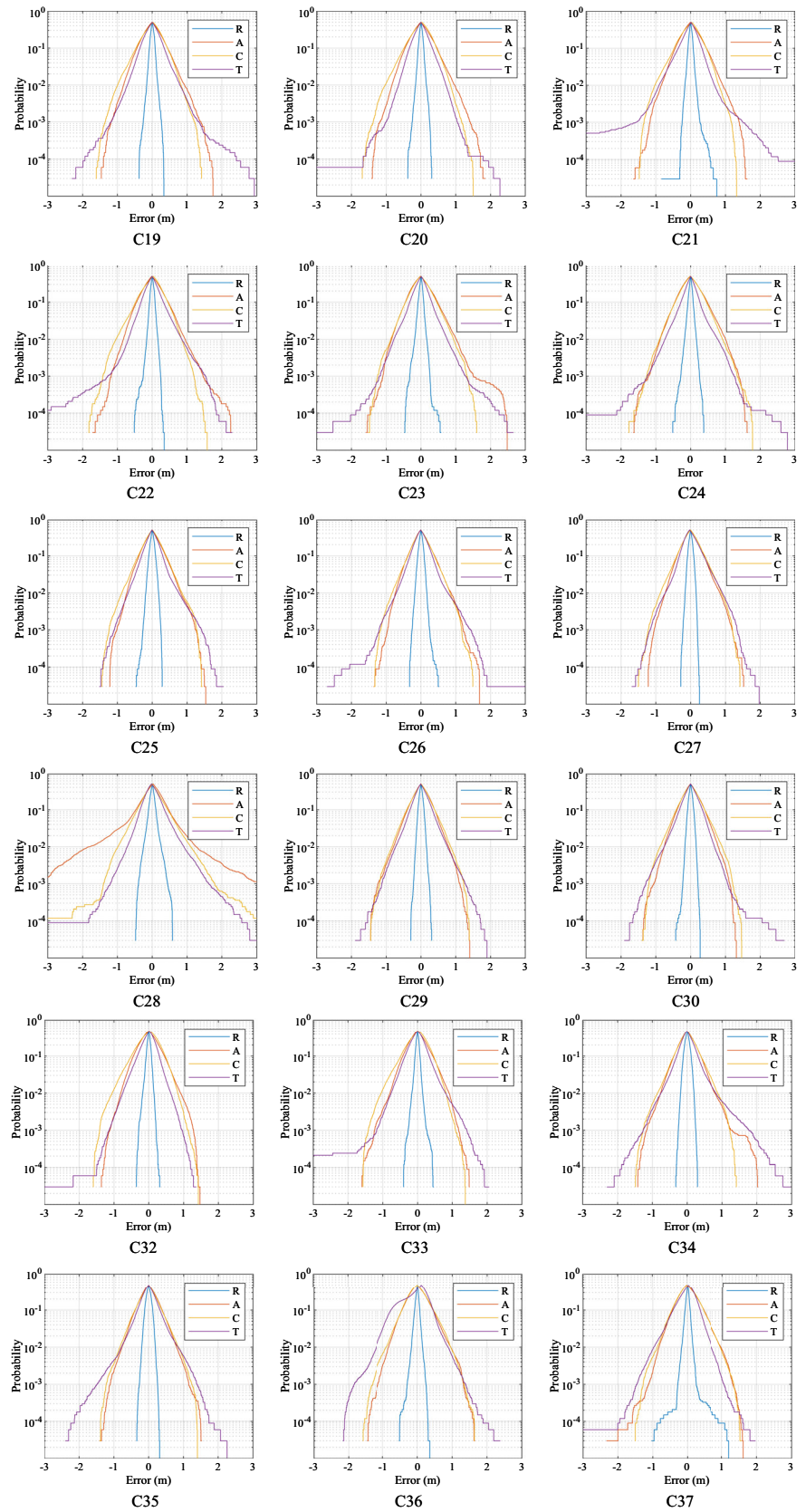


Fig. 5 Bounding the user-grid UREs in the form of FCDF for various satellites

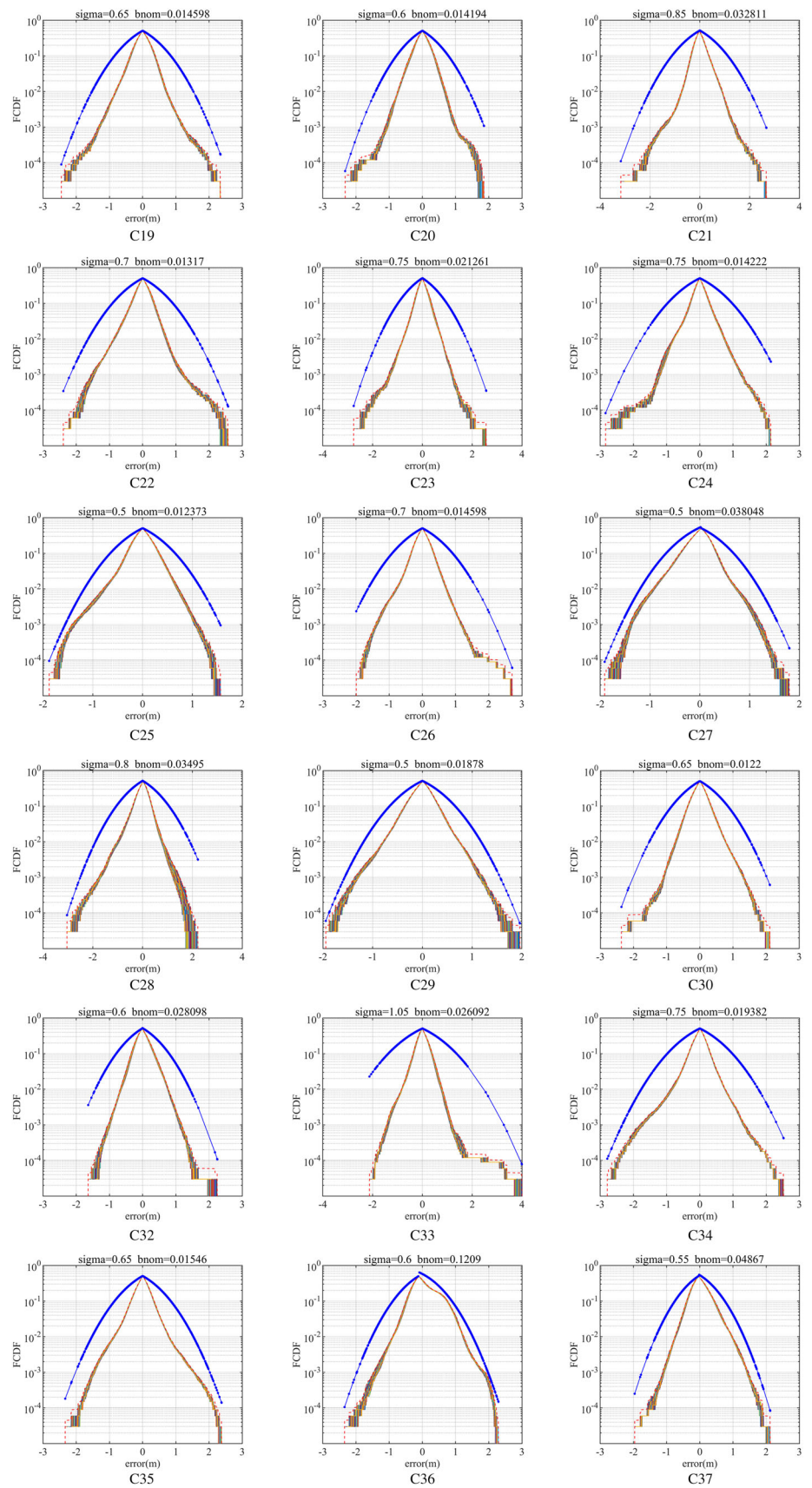


Table 4 σURA and fault probability of BDS-3 satellite

PRN	Orbit	Threshold (m)	URA (m)	b_{norm}	P_{sat}
C19	MEO	2.5	0.65	0.014598	11.9750e-05
C20	MEO	2.5	0.60	0.014194	5.9992e-05
C21	MEO	3.5	0.85	0.032811	5.6699e-05
C22	MEO	3.0	0.70	0.01317	1.4953e-05
C23	MEO	3.0	0.75	0.021261	2.9928e-05
C24	MEO	3.0	0.75	0.014222	8.9334e-05
C25	MEO	2.0	0.50	0.012373	2.9781e-05
C26	MEO	3.0	0.70	0.014598	2.9845e-05
C27	MEO	3.0	0.50	0.038048	2.9915e-05
C28	MEO	3.5	0.80	0.03495	9.0150e-05
C29	MEO	3.5	0.5	0.01878	2.0949e-05
C30	MEO	2.5	0.65	0.0122	5.9907e-05
C32	MEO	2.5	0.60	0.028098	2.9947e-05
C33	MEO	4.0	1.05	0.026092	11.935e-05
C34	MEO	3.0	0.75	0.019382	2.9771e-05
C35	MEO	2.5	0.65	0.01546	5.9857e-05
C36	MEO	2.5	0.60	0.1209	2.9891e-05
C37	MEO	2.5	0.55	0.04867	5.9873e-05

Subsequently, a comparison of SIS performance across different satellites was conducted. The estimated URA (σURA) of all monitored satellites is illustrated in Fig. 5, with the corresponding fault probability presented in Table 4. It is evident from the results that the σURA of most BDS-3 satellites ranges from 0.5 to 0.85 m, except C33, which has a larger value of over 1 m. The fault probabilities exhibit significant variations, spanning from 1.4953×10^{-5} (C22) to 1.1975×10^{-4} (C19). Note that these figures show variations using fault definitions and different thresholds, but it remains unknown which set of results best describes the long-term planned behavior. It is an open question for future study.

The results show that the SIS accuracy of the BDS-3 satellite is better than that of the BDS-2 satellite. For BDS-3 (B1C/B2a), σURA is about 0.5 to 0.85 m, while σURA of BDS-2 is about 2.4–3.2 m, σURA of BDS-3 (B3I) is about 1 m, far less than the accuracy index 2 m, specified in the official document [1]. The fault probability ranges from 1.5×10^{-5} to 1.2×10^{-4} for BDS-3 (B1C/B2a), while fault probability ranges from 1.3×10^{-4} to 1×10^{-3} for BDS-2, 4×10^{-5} to 3.5×10^{-4} for BDS-3 (B3I) [19]. It can be deduced that the performance of BDS-3 is better than that described in official documents. For developers of navigation application systems, the complexity of system design is reduced. For users, they can use BDS-3 with more peace of mind.

5 Conclusion

In this paper, the SIS performance of BDS-3 B1C and B2a was characterized from an integrity perspective. The data of BDS-3 over a 1-year period in 2021 are analyzed using CNAV, and then, the orbital error, clock error, SISRE, and fault probabilities are evaluated. The principal contribution of this study is the derivation of a clock error correction equation for the B1C/B2a dual-frequency combination. Also, we have assessed the SISRE of B1C/B2a, following a data-driven SISRE evaluation methodology under aviation safety standards. The results of this study show that:

- 1) The process of calculating the SISREs entails the comparison of broadcast satellite positions and clock offsets derived from CNAV with the precise products furnished by the IGS. The DCB parameters retrieved from IGS are selected to facilitate the conversion of the reference point for precise satellite clock offset from the APC of B1I + B3I ionospheric free to the APC of B1C + B2a ionospheric free.
- 2) BDS-3 MEO satellites have σURA of 0.5 to 0.85 m, and the overall accuracy is better than that of BDS-2 and comparable to that of GPS. The fault probability of BDS-3 MEO satellites is lower than that of BDS-2. The results have contributed to the application of BDS-3 in civil aviation and other safety-critical applications.

Acknowledgements This work was supported by the National Natural Science Foundation of China (Grant No. 62103274).

Funding This research was funded by National Natural Science Foundation of China (Grant No. 62103274).

Data availability Data openly available in a public repository.

Declarations

Conflict of interest The authors have not disclosed any competing interests.

References

- China Satellite Navigation System Management Office (2021) BeiDou Navigation Satellite System Open Service Performance Standard (version 3.0). <http://m.beidou.gov.cn/xt/gfxz/202105/P020210526216231136238.pdf>. Accessed 26 May 2021
- Yang Y, Gao W, Guo S (2019) Introduction to BeiDou-3 navigation satellite system. *Navigation* 66(1):7–18. <https://doi.org/10.1002/navi.291>
- The State Council Information Office of the People's Republic (2022) China's BeiDou Navigation Satellite System in the New Era. https://english.www.gov.cn/archive/whitepaper/202211/04/content_WS63647de9c6d0a757729e249d.html. Accessed 4 Nov 2022
- China Satellite Navigation System Management Office (2017) BeiDou navigation satellite system signal in space interface control document open service signal B1C (version 1.0). <http://www.beidou.gov.cn/xt/gfxz/201712/P020171226741342013031.pdf>. Accessed 27 Dec 2017
- China Satellite Navigation System Management Office (2017) BeiDou navigation satellite system signal in space interface control document open service signal B2a (version 1.0). <http://www.beidou.gov.cn/xt/gfxz/201712/P020171226742357364174.pdf>. Accessed 27 Dec 2017
- China Satellite Navigation System Management Office (2017) BeiDou navigation satellite system signal in space interface control document satellite based augmentation system service signal BDSBAS-B1C (version 1.0). <http://www.beidou.gov.cn/xt/gfxz/202008/P020200803362065480963.pdf>. Accessed 3 Aug 2020
- Wu Y, Liu X, Liu W, Ren J (2017) Long-term behavior and statistical characterization of BeiDou signal-in-space errors. *GPS Solutions* 21(4):1907–1922. <https://doi.org/10.1007/s10291-017-0663-0>
- Walter T et al (2019) Standards for ARAIM ISM Data Analysis. Pacific PNT Meeting, Honolulu, Hawaii, 777–784. <https://doi.org/10.33012/2019.16837>
- Blanch J et al (2015) Baseline advanced RAIM user algorithm and possible improvements. *IEEE Trans Aerosp Electron Syst* 51(1):713–732. <https://doi.org/10.1109/TAES.2014.130739>
- Zhai Y et al (2020) An advanced receiver autonomous integrity monitoring (ARAIM) ground monitor design to estimate satellite orbits and clocks. *J Navig* 73(5):1087–1105. <https://doi.org/10.1017/S0373463320000181>
- Wang S et al (2023) Implementation and analysis of fault grouping for multi-constellation advanced RAIM. *Adv Space Res* 71(11):4765–4786. <https://doi.org/10.1016/j.asr.2023.01.020>
- Walter T, Gunning K, Eric Phelts R, Blanch J (2018) Validation of the unfaulted error bounds for ARAIM. *Navigation* 65(1):117–133. <https://doi.org/10.1002/navi.214>
- Walter T, Blanch J, Joerger M (2019) Determination of fault probabilities for ARAIM. *IEEE Trans Aerosp Electron Syst* 55(6):3505–3516. <https://doi.org/10.1109/TAES.2019.2909727>
- Martini I, Sgammini M, Boyero JP (2020) Galileo model of group delay accuracy for advanced RAIM users. *Navigation* 67(1):129–141. <https://doi.org/10.1002/navi.356>
- Montenbruck O, Schmid R, Mercier F, Steigenberger P (2015) GNSS satellite geometry and attitude models. *Adv Space Res* 56(6):1015–1029. <https://doi.org/10.1016/j.asr.2015.06.019>
- Montenbruck O, Steigenberger P, Hauschild A (2018) Multi-GNSS signal-in-space range error assessment-methodology and results. *Adv Space Res* 61(12):3020–3038. <https://doi.org/10.1016/j.asr.2018.03.041>
- Xue B et al (2021) Performance of BeiDou-3 signal-in-space ranging errors: accuracy and distribution. *GPS Solution* 25(1):23. <https://doi.org/10.1007/s10291-020-01057-z>
- Chen G et al (2021) Statistical characterization of the signal-in-space errors of the BDS: a comparison between BDS-2 and BDS-3. *GPS Solution* 25(3):112. <https://doi.org/10.1007/s10291-021-01150-x>
- Wang S, Zhai Y, Zhan X (2021) Characterizing BDS signal-in-space performance from integrity perspective. *Navigation* 68:157–183. <https://doi.org/10.1002/navi.409>
- Steigenberger P, Montenbruck O, Hessels U (2015) Performance evaluation of the early CNAV navigation message. *Navigation* 62:219–228. <https://doi.org/10.1002/navi.111>
- Wang N, Yuan Y, Li Z et al (2016) Determination of differential code biases with multi-GNSS observations. *J Geod* 90:209–228. <https://doi.org/10.1007/s00190-015-0867-4>
- Wang X, Du Y (2018) BDT performance and time offset analysis. *J Phys*. <https://doi.org/10.1088/1742-6596/1060/1/012003>
- Wei Z et al (2008) China geodetic coordinate system 2000 and its comparison with WGS84. *J Geod Geodyn* 28(5):1–5. <https://doi.org/10.4028/www.scientific.net/AMM.580-583.2793->
- Yang Y et al (2019) Introduction to BeiDou-3 navigation satellite system. *Navig J Inst Navig* 66(1):7–18. <https://doi.org/10.1002/navi.291>
- Warren D, Raquet J (2003) Broadcast vs. precise GPS ephemerides: a historical perspective. *GPS Solutions* 7(3):151–156. <https://doi.org/10.1007/s10291-003-0065-3>
- Montenbruck O, Steigenberger P, Hauschild A (2015) Broadcast versus precise ephemerides: a multi-GNSS perspective. *GPS Solutions* 19(2):321–333. <https://doi.org/10.1007/s10291-014-0390-8>
- Montenbruck O et al (2015) GNSS satellite geometry and attitude models. *Adv Space Res* 56(6):1015–1029. <https://doi.org/10.1016/j.asr.2015.06.019>
- Larson J (2018) Gaussian-Pareto Overbounding: A Method for Managing Risk in Safety-Critical Navigation Systems (Doctoral dissertation)
- Zhao Q et al (2018) Precise orbit and clock determination for BeiDou-3 experimental satellites with yaw attitude analysis. *GPS Solutions*. <https://doi.org/10.1007/s10291-017-0673-y>
- Zhao Q et al (2022) Precise orbit determination for BDS satellites. *Satellite Navig*. <https://doi.org/10.1186/s43020-021-00062-y>

Springer Nature or its licensor (e.g. a society or other partner) holds exclusive rights to this article under a publishing agreement with the author(s) or other rightsholder(s); author self-archiving of the accepted manuscript version of this article is solely governed by the terms of such publishing agreement and applicable law.